Int. J. Electrochem. Sci., 14 **(2019)** 11325 – 11339, doi; 10.20964/2019.12.43

International Journal of ELECTROCHEMICAL SCIENCE
www.electrochemsci.org

Effects of Operating Parameters on Electrochemical Treatment of Swine Wastewater

Kuo-Lin Huang[1,], Chou-Ching Liu[1], Chen-Yao Ma[2], Tien-Tien Chen[3]*

[1] Department of Environmental Science and Engineering, National Pingtung University of Science and Technology, Pingtung 91201, Taiwan (R.O.C.)
[2] Environmental Protection Bureau, Kaohsiung City Government, Kaohsiung 83347, Taiwan (R.O.C.)
[*]E-mail: huangkl@mail.npust.edu.tw
[3] Prosperity Sci-Tech Co., Ltd., Taipei 10067, Taiwan (R.O.C.)

Received: 3 July 2019 / *Accepted:* 17 September 2019 / *Published:* 29 October 2019

This study focuses on the electrochemical treatment of swine wastewater under different parameters (anode material, cathode distance, cathode area, and wastewater volume). The results showed that for a total of 16 tests, the pseudo-first-order COD and NH_3-N removal rate constants ranged from 9.00×10^{-5}–5.98×10^{-4} and 5.66×10^{-5}–1.45×10^{-3} 1/s, respectively, with removal efficiencies of 79%–100% and 72%–100%, respectively. The range of specific energy consumption (E_{SP}) was 32–358 kWh/kg-COD. The performance of a lab-prepared boron-doped diamond (BDD) anode was comparable to that of a commercial anode for the electrochemical removal of COD and NH_3-N in swine wastewater. Among tested anode materials, IrO_2/Ta_2O_5 exhibited the lowest performance in terms of COD and NH_3-N removal, and BDD showed better COD degradation performance than PbO_2 although an opposite trend was observed for NH_3-N removal. The COD and NH_3-N removal efficiencies increased as the electrode distance increased. Increasing the cathode area also increased the removal efficiency of pollutants and was beneficial for controlling the final pH. Of all the tests, the lowest E_{SP} (32 kWh/kg-COD) was obtained by increasing the wastewater volume and lowering the current density, which can be considered for energy or cost savings related to operation.

Keywords: swine wastewater; electrochemical degradation; anode material; electrode distance; cathode area

1. INTRODUCTION

To meet the increasing demand for pork associated with population growth, intensive, large-scale pig feeding operations have been developed in several nations, including the United States [1] and some European and Asian countries [2], especially China [3], leading to an increasing discharge of swine wastewater and increased concern related to adverse impacts on the environment and human

health [1−3]. In addition to suspended solids pathogens, heavy metals, antimicrobials, and hormones, high levels of organic total-nitrogen and total-phosphorus related compounds are of great concern, and regulated water quality parameters for piggery wastewater treatment and discharge are needed [1,4−6].

Different methods have been studied and used for the removal of the organic matter and nutrients in swine wastewater. Traditionally, swine wastewater is typically treated using biological processes before discharge or reuse as fertilizers for agricultural purposes [4]. Therefore, swine wastewater is commonly treated by the initial physical separation of solids from the liquid manure, then by aerobic digestion for organic pollutant degradation and methane recovery, and lastly by nitrification/denitrification for nitrogen removal [7,8]. Although this three-step process is time-consuming, it has also been adopted for swine wastewater treatment in Taiwan [9]. Chemical coagulation is also effective at separating solids and liquids in livestock wastewater [4]; however, it is not popular. Recently, chemical coagulation was also tested for swine slaughterhouse wastewater treatment, but it suffered from low turbidity and color removal with <90% chemical oxygen demand (COD) degradation [10]. To alleviate swine wastewater pollution, it is necessary to develop more efficient approaches for swine wastewater treatment.

The highly reactive hydroxyl radical (•OH) generated in the electrochemical advanced oxidation process (EAOP) is a powerful method that can be used to remove organic pollutants in wastewater. In addition, the EAOP, relying on electrochemically generated active chlorine, also has good potential for efficient degrading nitrogen-containing compounds in wastewater [11−14]. In the EAOP, non-active anode materials (e.g., RuO_2, PbO_2, and BDD) can be used to effectively produce •OH for COD degradation [11−13] and generate active chlorine for ammonia nitrogen removal [14]. However, little attention has been paid to electrochemical removal of organic and ammonia pollutants in swine wastewater. In our previous work, we preliminarily tested the removal of COD and ammonia in swine wastewater at different electrolyte types, current densities, and anode areas [15]. In this study, we further explored the effects of different operating parameters (anode material, cathode distance, cathode area, and wastewater volume) on the removal of organic and ammonium nitrogen pollutants in swine wastewater using the EAOP.

2. MATERIALS AND METHODS

2.1. Collection and chemical analysis of swine wastewater

The swine wastewater samples tested in this study were collected from different pig farms in southern Taiwan. These samples were stored at 4^{o}C before use. Each wastewater sample was filtered using a 0.45 μm filter to remove suspend solids prior to testing. The analyses of chemical oxygen demand (COD), conductivity (EC), ammonium nitrogen (NH_3-N), nitrite nitrogen (NO_2^--N), nitrate nitrogen (NO_3^--N), and pH followed the methods set forth in the National Institute of Environmental Analysis (NIEA) W517.52B, W203.51B, W448.51B, W418.53C, W419.51B, and W424.52A, respectively, from the Environmental Protection Administration (EPA), Taiwan.

The chemical oxygen demand (COD) was analyzed using a COD analyzer (COD Reactor CR25, Rocker) coupled with a colorimeter (Hach-DR900). A Gerhardt VAP-200 Kjeldahl Nitrogen Distillation System was used to achieve the required digestion for the ammonia measurements. The photometric determination of NH_3-N at 640 nm (Hitachi U-2900) was based on the reaction of ammonia with phenol and hypochlorite catalyzed with nitroprusside to form intensively blue indophenol in an alkaline medium (Berthelot reaction). Some ammonia measurements were also conducted using a Hach-DR900 analyzer.

The NO_2^--N of a sample was diazotized with sulfanilamide followed by coupling with N-(1-naphthyl)-ethylenediamine dihydrochloride (NED), and the concentration of nitrite was then spectrophotometrically measured at 543 nm. Nitrate was determined by using its absorbance at 220 nm through deduction of the double absorbance at 275 nm for each sample. A redox potential titrator (Metrohm 702 SM Titrino) was used to quantitatively determine the chloride concentration, while the pH and EC were measured using a TS-100 pH meter and an SC-170 conductivity meter (Suntex, Taiwan), respectively.

2.2. Electrolytic removals of organic and NH_3-N pollutants

The removal of aqueous organic and NH_3-N pollutants was tested under different operating conditions (anode substance, electrode distance, cathode area, and wastewater volume). The electrolysis of swine wastewater with the addition of 0.05 M NaCl was carried out in an undivided electrochemical cell at 25ºC and 0.25 A/cm^2. In this study, we tested five different anode materials: boron-doped diamond (BDD on Nb (BDD-I) (Neocoat, Germany)) and lab-prepared materials (Nb/BDD (BDD-II), graphite/PbO_2, and Ti/PbO_2), and IrO_2/Ta_2O_5 dimensionally stable anode (DSA), whereas the cathode was a Ti plate. The fabrication method for the lab-prepared PbO_2 was provided elsewhere [16], while in the case of the lab-prepared BDD-II referred to hot filament chemical vapor deposition (HFCVD) [17]. All the electrolytic experiments were performed using a DC power supply (Twintex TP2H-20S, Taiwan,) which monitored the cell voltage and current over time.

The degradation or removal efficiency of COD or NH_3-N was calculated using the following equation:

$$\text{Degradation or removal efficiency} = ((1 - C_t/C_0)\times 100\%) \quad (1)$$

where C_t is the residual concentration of either COD or NH_3-N at a given electrolysis time t and C_0 is the initial concentration of COD or NH_3-N.

The specific energy consumption (E_{SP}) (kWh/kg-COD) was determined using the following calculation [12,18]:

$$E_{SP} = UIt/(COD_0 - COD_t)V_W \quad (2)$$

where U is the average cell voltage; I is the applied current (A); V_W is the wastewater volume (L); and COD_0 and COD_t are COD values measured at time t = 0 and t (in g O_2/L), respectively,.

3. RESULTS AND DISCUSSION

3.1. Characteristics of swine wastewater

The concentrations of COD, NH_3-N, NO_2^--N, NO_3^--N, and Cl^- (mg/L) in the raw swine wastewater samples (A1, A2, B1, B2, and C) ranged from 910−6200, 86−700, 0.01−3.71, 0.48−61.8, and 354−975 mg/L, respectively, while those for conductivity (EC) and pH ranged from 2.01−7.08 ms/cm and 7.33−7.93, respectively (Table 1). After the addition of 0.05 M NaCl, the EC values of the samples increased by 5−6 ms/cm.

Table 1. Concentrations of COD, NH_3-N, NO_2^--N, NO_3^--N, Cl^- (mg/L), EC (ms/cm), and the pH of the raw swine wastewater samples.

Wastewater	COD	NH_3-N	NO_2^--N	NO_3^--N	Cl^-	EC	pH
A1	1025	86	0.01	0.48	975	2.01	7.33
A2	910	126	3.71	23.6	532	2.47	7.84
B1	6200	700	0.02	61.8	413	7.08	7.78
B2	3300	248	0.01	25.2	354	3.35	7.68
C	1560	491	0.51	23.8	445	4.83	7.93

3.2. Effect of anode substance on COD, NH_3-N, NO_2^--N, and NO_3^--N removals

Anode substances play a key role in pollutant degradation using electrochemical advanced oxidation processes (EAOPs). In this study, five different anodes (BDD-I, BDD-II, graphite/PbO_2, Ti/PbO_2, and DSA) were tested. According to Figure 1a, the performance of these anodes was in the following order: BDD-I ≈ BDD-II > graphite/PbO_2 ≈ Ti/PbO_2 > DSA in terms of COD removal efficiency (100%, 100%, 97%, 97%, and 90% at 150, 180, 240, 240, and 240 min, respectively), with a pseudo-first-order rate constant ($k = (5.98-1.48)\times10^{-4}$ 1/s) and specific energy consumption (E_{SP}) (97−358 kWh/kg-COD) (Table 2). These findings were similar to those of several studies for organic pollutant abatement in wastewater [11,19−21] mainly because the oxygen evolution potential was higher on BDD (2.2−2.6 V vs. SHE) than on PbO_2 (1.8−2.0 V vs. SHE) and IrO_2/Ta_2O_5 DSA (1.5−1.8 V vs. SHE) [11,22]. More importantly, hydroxyl radicals (•OH) can be electrochemically generated to a much greater degree on non-active electrodes (E) (e.g., BDD and PbO_2) than on active electrodes (e.g., DSA and Pt) via Eq. 3; furthermore, •OH may be used for the degradation or mineralization of organic pollutants (R) in solution through Eq. 4 [23].

$$E + H_2O \rightarrow E(\bullet OH) + H^+ + e^- \quad (3)$$

$$E(\bullet OH) + R \rightarrow M + mCO_2 + nH_2O + H^+ + e^-, \quad (4)$$

where the values of *m* and *n* depend on the elemental composition of the R to be oxidized. Therefore, it can be inferred that the electrochemical generation of •OH was more favorable on BDD than on PbO_2, similar to the observations reported in the literature [11,19,20].

Dissimilarly, the anode performance for NH_3-N removal in swine wastewater changed to the following order: graphite/PbO_2 ≈ Ti/PbO_2 > BDD-I ≈ BDD-II > DSA (Figure 1b), consistent with the electrolysis time required for 100% NH_3-N removal using these anodes (30, 60, and 90 min for PbO_2, BDD, and DSA, respectively). Note that the electrolysis time for complete removal was shorter for NH_3-N than for COD. However, the NH_3-N removal performance was observed to be similar on BDD and PbO_2 in our earlier study, and the removal of NH_4^+ in sanitary landfill leachates has also been reported to be similar on these two types of anodes [24]. The k values for these anodes decreased from 1.45×10^{-3} to 1.85×10^{-4} 1/s (Table 2). A previous work also reported the pseudo first-order kinetics [25]. Therefore, the formation of active chlorine (e.g., Cl_2, HOCl, and OCl^-) (effective for NH_3-N removal) from chloride oxidation should be more favorable on PbO_2 than on BDD since the chloride concentrations were similar in the solutions used for the anode tests.

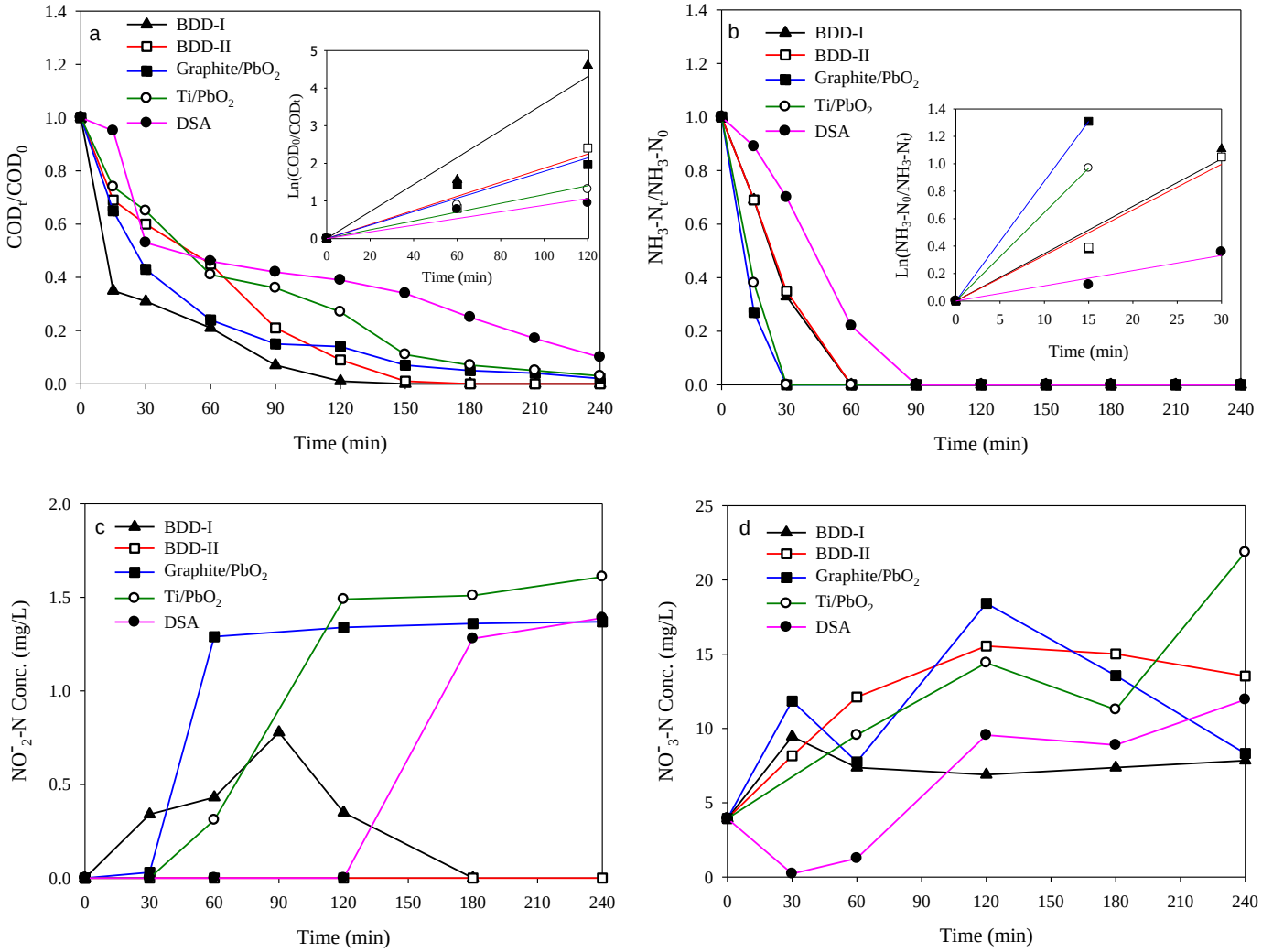

Figure 1. Concentration variations in COD (a), NH_3-N (b) NO_2^--N (c), and NO_3^--N (d) over time for different anode materials during electrochemical treatment of swine wastewater at 25°C and 0.25 A/cm^2 (d = 2.6 cm and CA = 4 cm^2) (inset: Ln(C_0/C) against time, C = COD or NH_3-N).

It is known that both indirect (mediated) and direct electrochemical reactions may cause the removal of NH_3-N on BDD or PbO_2 in water or wastewater [13,14,26−29]. In the presence of chloride, active chlorine can be electro-generated based on the following reactions [26]:

$$2Cl^- \rightarrow Cl_2 + 2e^- \quad (5)$$

$$Cl_2 + H_2O \rightarrow HClO + H^+ + Cl^- \quad (6)$$

$$HOCl \rightarrow OCl^- + H^+ \quad (7)$$

The produced HOCl can be used to oxidize NH_3 or NH_4^+ via reactions 9−12 [14] or to form chloramines [26,28], although the formation of chloramines is insignificant at pH > 8 [28].

$$3HOCl + 2NH_3 \rightarrow N_2 + 3H_2O + 3H^+ + 3Cl^- \quad (8)$$

$$3HOCl + 2NH_4^+ \rightarrow N_2 + 3H_2O + 5H^+ + 3Cl^- \quad (9)$$

$$4HOCl + NH_4^+ \rightarrow NO_3^- + H_2O + 6H^+ + 4Cl^- \quad (10)$$

$$4OCl^- + NH_3 \rightarrow NO_3^- + H_2O + H^+ + 4Cl^- \quad (11)$$

Table 2. Tests (denoted by operating parameters), wastewater (W), electrolytic time (t, min), pseudo-first-order rate constants (k, 1/s), removal efficiencies (R_E, %), and specific energy consumption (E_{SP}, kWh/kg-COD) of COD degradation and NH_3-N removal on BDD for the tested swine wastewater (G: graphite, d: electrode distance, C_A: cathode area, V_W: wastewater volume, and C_D: current density).

Test	W	COD				NH_3-N		
		t	k	R_E	E_{SP}	t	k	R_E
BDD-I	A1	150	5.98×10^{-4}	100	97	60	5.75×10^{-4}	100
BDD-II		180	3.11×10^{-4}	100	261	60	5.53×10^{-4}	100
G/PbO_2		240	2.98×10^{-4}	97	208	30	1.45×10^{-3}	100
Ti/PbO_2		240	1.95×10^{-4}	97	302	30	1.07×10^{-3}	100
DSA		240	1.48×10^{-4}	90	358	90	1.85×10^{-4}	100
d-0.4 cm	A2	240	2.10×10^{-4}	97	131	90	2.91×10^{-4}	100
d-1.5 cm		240	4.33×10^{-4}	99	113	90	3.78×10^{-4}	100
d-2.6 cm		240	5.01×10^{-4}	99	124	60	4.18×10^{-4}	100
CA-4 cm^2	B1	240	1.21×10^{-4}	94	72	240	1.33×10^{-4}	100
CA-2 cm^2		240	1.16×10^{-4}	83	108	240	9.66×10^{-5}	79
CA-1 cm^2		240	9.00×10^{-5}	79	174	240	6.33×10^{-5}	72
CA-8 cm^2	B2	240	2.68×10^{-4}	96	95	150	2.08×10^{-4}	100
CA-4 cm^2		240	2.46×10^{-4}	93	109	150	1.81×10^{-4}	100
CA-2 cm^2		240	1.90×10^{-4}	90	184	150	1.65×10^{-4}	100
V_W -200 mL C_D-0.25 A/cm^2	C	240	2.01×10^{-4}	95	213	240	1.40×10^{-4}	89
V_W -1000 mL C_D-0.05 A/cm^2		240	1.88×10^{-4}	90	32	240	5.66×10^{-5}	79

Through transfer of 6 electrons, the direct (non-mediated) electrochemical oxidation of ammonia on tested anodes may occur as the following equation:

$$2NH_3 \rightarrow N_2 + 6H^+ + 6e^- \quad (12).$$

The concentration of nitrite for BDD-I initially increased, then decreased after 90 min, and finally became undetectable (ND) at 180 min. However, the concentration of nitrite for BDD-II was

ND during the electrolysis of wastewater (Figure 1c). When PbO_2 anodes were used, nitrite was not detected initially, and subsequently, its concentration increased with increases in electrolysis time, but this increase in the nitrite concentration became smaller after 30 and 120 min for graphite/PbO_2 ≈ Ti/PbO_2, respectively. This trend was also observed for DSA; nevertheless, nitrite was not detected before 120 min. The lower formation of nitrite for BDD than for PbO_2 is similar to the observation indicating that ammonium is more favorably oxidized to nitrate on BDD than on PbO_2 in sanitary landfill leachates [24].

At low concentrations (< 2 mg/L as NO_2^--N), nitrite may be produced from the electrochemical oxidation of ammonia on the anode (Eq. 20) or the electrochemical reduction of nitrate on the cathode (Eq. 21 [30]):

$$NH_4^+ + 2H_2O \rightarrow NO_2^- + 8H^+ + 6e^- \quad (13)$$

$$NO_3^- + H_2O + 2e^- \rightarrow NO_2^- + 2OH^- \quad (14)$$

On the other hand, the following reaction may reduce the accumulation of nitrite in the wastewater [28]:

$$NO_2^- + OCl^- \rightarrow NO_3^- + Cl^- \quad (15)$$

The concentrations of nitrate initially increased to maximums and then decreased over time in the case of the BDD and PbO_2 anodes. An opposite trend was observed when using the DSA anode (Figure 1d). This finding accompanied with detected low nitrite concentrations supports the premise that the direct or indirect electrochemical generation of nitrate was faster than the formation of nitrite (Eq. 21), and/or nitrate was partially converted into nitrogen gas by active chlorine or was electrochemically reduced via the following reaction [31].

$$2NO_3^- + 12H^+ + 10e^- \rightarrow N_2 + 6H_2 \quad (16)$$

Based on the discussion in this section, BDD-I was chosen for the subsequent electrolytic experiments.

3.3. Effect of electrode distance on COD, NH_3-N, NO_2^--N, and NO_3^--N removals

The distance or spacing between the anode and cathode may influence organic pollutant degradation performance [32]. In this study, three electrode distances (d = 0.4, 1.5, and 2.6 cm) were tested for COD and NH_3-N removal on BDD. It was found that the COD (97−99%) and NH_3-N removal efficiencies (100% for d = 0.4, 1.5, and 2.6 cm at 60, 60, and 90 min, respectively) increased with increases in the electrode distance (Figures 2a and b, respectively) (Table 2). This phenomenon was partially attributed to the greater cell voltage and thus the anode overpotential at the longer electrode distance, which is more advantageous for pollutant degradation. However, a previous study reported an opposite trend for the electrolysis of nicosulfuron on a Ti/Ta_2O_5-IrO_2 electrode [32]. The difference in anode material should be responsible for the different results obtained in different works.

The E_{SP} for d = 1.5 cm was 113 kWh/kg-COD, lower than those for d = 0.4 and 2.6 cm (131 and 124 kWh/kg-COD, respectively), revealing the trade-off between cell potential and COD removal. The k values of COD and NH_3-N removal for increasing electrode distances increased from 2.10×10^{-4} to 5.01×10^{-4} 1/s and from 2.91×10^{-4} to 4.18×10^{-4} 1/s, respectively, although pseudo zero-order kinetics

might also be considered for the NH_3-N removal because its degradation curves in Figure 2b appear to be linear (Table 2). Pseudo zero-order kinetics for the electrochemical oxidation of ammonia with chlorine has also been suggested by some researchers [33,14].

The nitrite concentration variations for d = 2.6 cm were similar to those for d = 1.5 cm, but they differed from those for d = 0.4 cm, which had nitrite concentrations below the detection limit at 120 min, one-half that of d = 2.6, or 1.5 cm (240 min) (Figure 2c). Similar nitrate concentration variation curves were observed over time, while the lowest nitrate concentration was obtained at d = 2.6 cm among the tests (Figure 2d). Also, based on the COD and NH_3-N removal performance, d = 2.6 cm was used in the subsequent experiments.

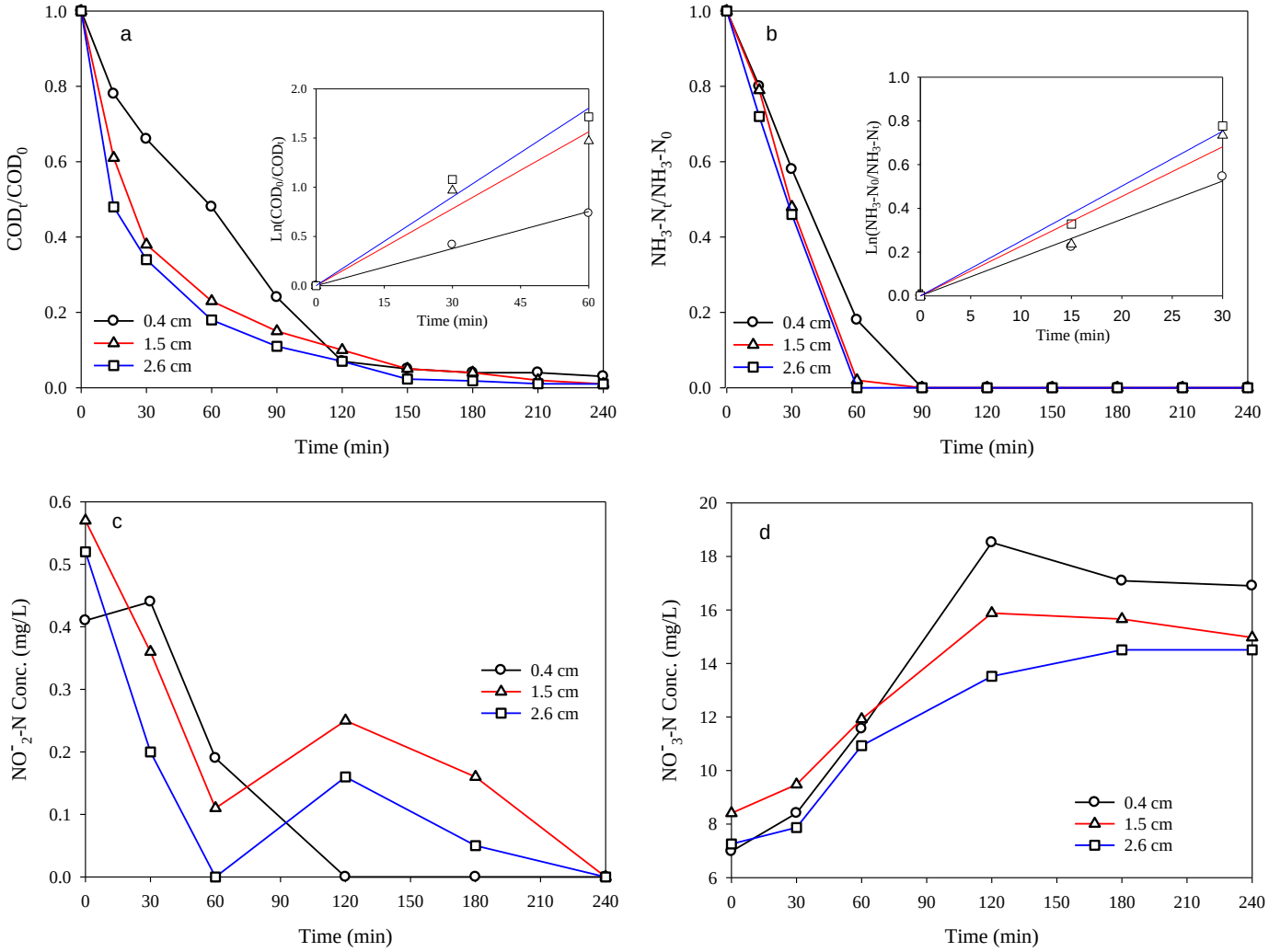

Figure 2. Concentration variations in COD (a), NH_3-N (b) NO_2^--N (c), and NO_3^--N (d) over time for different electrode distances during electrochemical treatment of swine wastewater at 25ºC and 0.25 A/cm^2 (anode: BDD-I and CA = 4 cm^2) (inset: Ln(C_o/C) against time, C = COD or NH_3-N)).

3.4. Effects of cathode area on COD, NH_3-N, NO_2^--N, and NO_3^--N removals and pH

The effects of cathode area on COD, NH_3-N, NO_2^--N, and NO_3^--N removal and pH at 0.25 A/cm^2 and 200 mL were tested using two batches (wastewater B1 and B2) (three runs per batch) for different cathode areas of 1−4 and 2−8 cm^2, respectively. Both batches showed increasing COD removal efficiency with increases in the cathode area (79−94% and 90−96% for 1−4 and 2−8 cm^2, respectively) (Figures 3a and b) (Table 2). Coincidently, the E_{SP} decreased with increases in the COD removal efficiency or cathode area (174−72 and 184−95 kWh/kg-COD for 1−4 and 2−8 cm^2, respectively). This result was associated with the fact that the increase of cathode area resulted in a decrease in cathode current density since the current was the same in each run. As a consequence, the reduction reactions on the cathode were weakened and thus indirectly increased COD removal because all the anodes had the same current density and area. Similarly, increased COD removal with increases in the cathode area from 16.5 to 50 cm^2 was also observed for the electrolysis of chloroform using a Ti/IrO2 anode and a Cu/Zn cathode in aqueous solution [34].

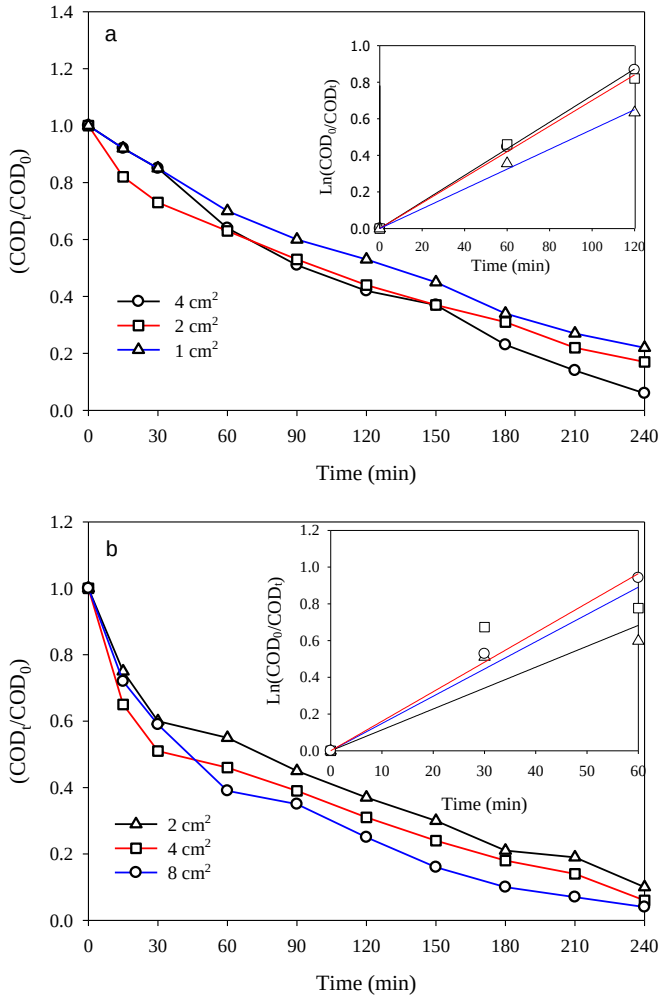

Figure 3. COD concentration variations over time for different cathode areas ((a) 1–4 cm^2 and (b) 2–8 cm^2) during electrochemical treatment of swine wastewater at 25ºC and 0.25 A/cm^2 (anode: BDD-I and d = 2.6 cm) (inset: Ln(C_o/C) against time, C = COD or NH_3-N).

A similar trend was also found for NH_3-N removal in the two test batches (Figures 4a and b). The ranges of NH_3-N removal efficiencies in these two batches were 72–100% and all-100%, respectively. Therefore, the above explanation is also applicable for NH_3-N removal for different cathode areas although the NH_3-N should be removed more by active chlorine rather than by •OH or direct anodic oxidation. The k values of COD removal for cathode areas of 1−4 and 2−8 cm^2 ranged from 9.00×10^{-5}–1.21×10^{-4} and from 1.90×10^{-4}–2.68×10^{-4} 1/s, respectively, while the corresponding data ranged from 6.33×10^{-5}–1.33×10^{-4} and 1.65×10^{-4}–2.08×10^{-4} 1/s, respectively, for NH_3-N removal (Table 2).

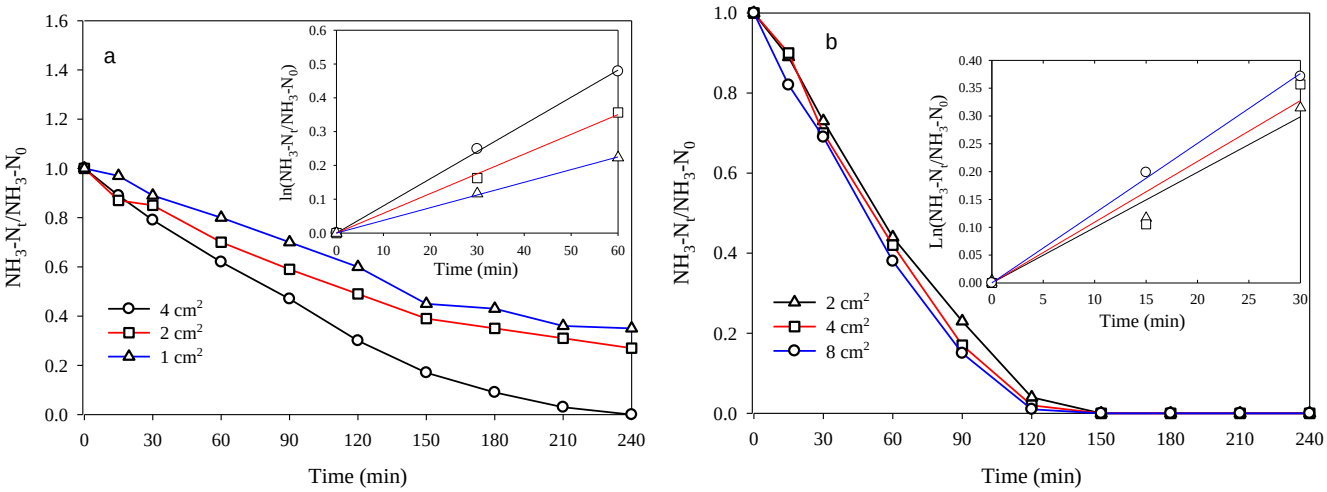

Figure 4. NH_3-N concentration variations over time for different cathode areas ((a) 1–4 cm^2 and (b) 2–8 cm^2) during electrochemical treatment of swine wastewater (at 25°C and 0.25 A/cm^2) (anode: BDD-I and d = 2.6 cm).

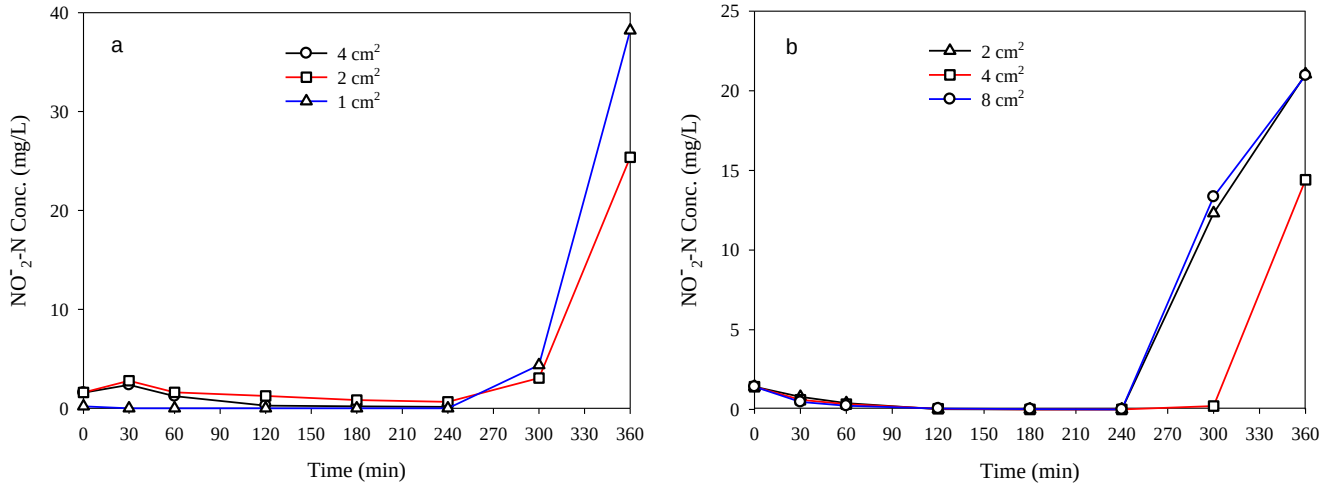

Figure 5. NO_2^--N concentration variations over time for different cathode areas ((a) 1–4 cm^2 and (b) 2–8 cm^2) during electrochemical treatment of swine wastewater (at 25°C and 0.25 A/cm^2) (anode: BDD-I and d = 2.6 cm).

In the batch B1 test, the nitrite concentration began to significantly increase after electrolysis for more than 240 min for cathode areas of 1 and 2 cm^2, while that for the cathode area of 4 cm^2

dropped to ND after 120-min of electrolysis and lasted to the end of electrolysis (240 min) (Figure 5a). This pattern also occurred in the batch B2 test, but a significant increase in the nitrite concentration was also observed starting after 240-min of electrolysis (Figure 5b).

It was noted that the nitrate concentration in each run increased to a maximum and then decreased over time in both the batch B1 and B2 tests (Figures 6a and b). Hence, the final products from NH_3-N removal should include nitrogen gas. The formation of nitrate increased with increases in the cathode area, so the trade-off between COD or NH_3-N removal and nitrate production requires evaluation to determine if nitrate concentration in addition to COD or NH_3-N concentration is regulated by effluent standards.

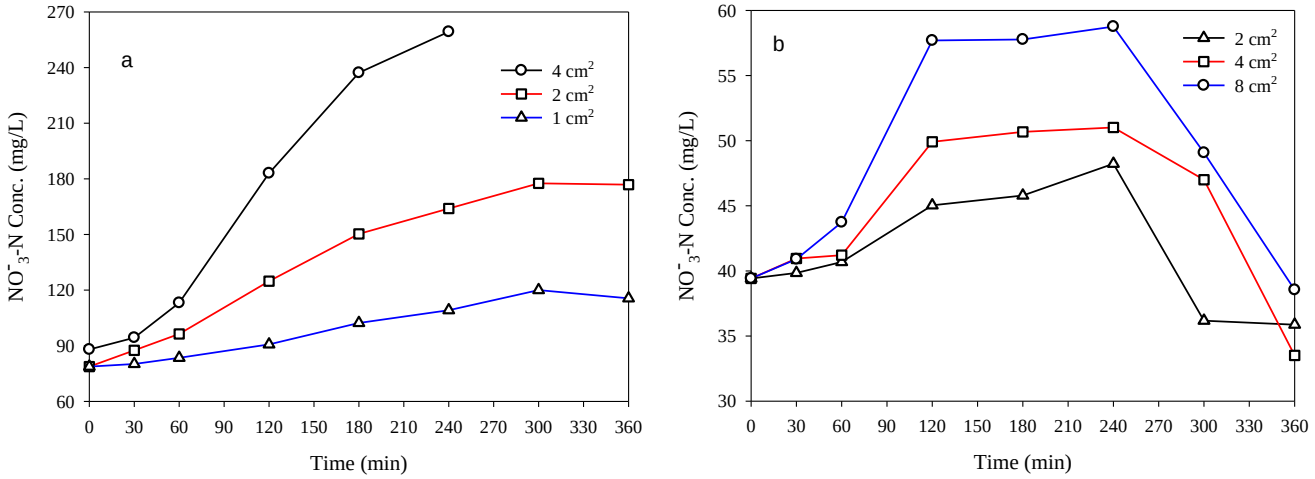

Figure 6. NO_3^--N concentration variations over time for different cathode areas ((a) 1–4 cm^2 and (b) 2–8 cm^2) during electrochemical treatment of swine wastewater (at 25°C and 0.25 A/cm^2) (anode: BDD-I and d = 2.6 cm).

Figure 7a shows the variations in pH over time when using the Ti cathodes with different areas of 1–4 cm^2 at a BDD anode area of 4 cm^2 in the batch B1 test. The pH values for cathode areas = 1 and 2 cm^2 initially decreased, reached a plateau, and finally significantly increased over time. The pH value for the cathode area of 4 cm^2 also decreased over time from the beginning (7.86), reached a minimum (4.68) at 180 min, and subsequently increased until the end of the 240-min electrolysis (5.76). All these runs, particularly for the cathode area = 4 cm^2, exhibited pH values at 240 min that were lower than their initial values although for cathode areas = 1 and 2 cm^2, the 360-min pH values (9.83 and 9.36, respectively) were higher than those at 0-min (7.58 and 7.63, respectively). At the same BDD anode area of 4 cm^2, a similar trend in pH variations over time was also shown for cathode areas = 2, 4, and 8 cm^2 in the batch B2 test (360-min pH = 10.31, 9.99 and 9.97, respectively) (Figure 7b). It is thus better to obtain pH values ranging from 6–9 in treated effluent to meet the general regulatory limit for effluent pH. In both batch tests, more initial pH decreases and less final pH increases were observed when using a smaller cathode area for the electrolysis of wastewater for 360 min. This result might be briefly associated with the main side reactions on the anode and cathode (water oxidation and reduction, respectively), which correspond to H^+ generation and OH^- production (or H^+ consumption), respectively. As mentioned earlier, the fact that the cathode current density was lower when the

cathode area was larger at the same current led to the less OH^- production or H^+ consumption in solution and thus the buildup of H^+, resulting in faster prior decrease and slower final increase in the pH value. Accordingly, electrolysis time influenced the final solution pH and it could also be adjusted by the anode/cathode ratio.

In addition to anode water oxidation and cathode water reduction, NH_3-N removal may affect solution pH (reactions 6–13), and vice versa. The pK_a values of $NH_4^+ \leftrightarrow NH_3$ and $HOCl \leftrightarrow OCl^-$ reactions were 9.24 and 7.50, respectively, which were in the solution pH ranges that occurred during wastewater electrolysis. A low pH is favored to form HOCl in $HOCl \leftrightarrow OCl^-$ transformation but is unfavorable for the formation of HOCl, as shown in Eq. 6 [14]. Although a low pH also adversely affects the removal of free ammonia (NH_3-N) and ionized-ammonia (NH_4^+-N) by active free chlorine, based on Eqs. 8–10, it has been reported that direct (non-mediated) electrochemical oxidation of ammonia on BDD proceeds largely at a high pH (> 8) via free ammonia (NH_3) oxidation (Eq. 12) [26]; nevertheless, it has been mentioned that neutral and alkaline pH are beneficial to ammonia oxidation [14].

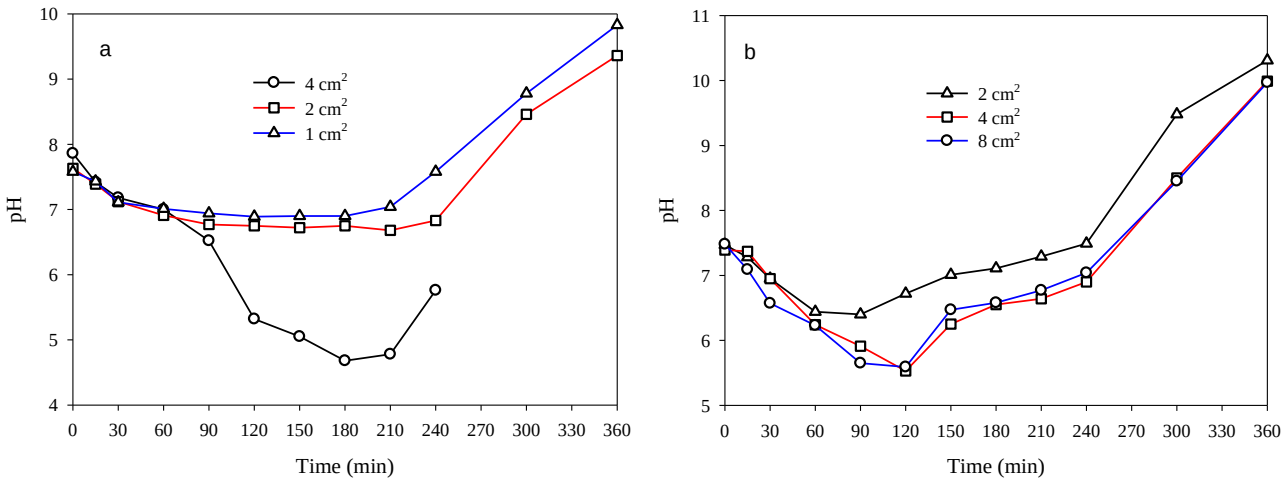

Figure 7. Variations in pH over time for different cathode areas ((a) 1–4 cm^2 and (b) 2–8 cm^2) during electrochemical treatment of swine wastewater (at 25°C and 0.25 A/cm^2) (anode: BDD-I and d = 2.6 cm).

3.5. Effect of wastewater volume on COD, NH_3-N, NO_2^--N, and NO_3^--N removals

For the purpose of practical use, COD and NH_3-N removal was also tested using a larger wastewater volume (V_W) of 1000 mL, while the total current and anode area/wastewater volume remained the same as than when using 200 mL swine wastewater (1 A and 4/200 (or 20/1000), respectively). Therefore, the conditions for wastewater volume = 1000 mL and current density (C_D) = 0.05 A/cm^2 against V_W = 200 mL and C_D = 0.25 A/cm^2 were compared. The former condition exhibited better COD removal efficiency than the latter one although their initial COD removal efficiencies were similar (Figure 8a). A similar tendency was also observed for their NH_3-N removal (Figure 8b). This result was attributed to the fact that the current density was higher, but the COD

amount was lower at V_W = 200 mL and C_D = 0.25 A/cm^2 than it was at V_W = 1000 mL and C_D = 0.05 A/cm^2, so the former had more generated •OH and active chlorine that could be used than the latter for COD and NH_3-N removal, respectively. For the 240-min electrolysis, the removal efficiencies of COD in these two tests were 95% and 90%, respectively, whereas those for NH_3-N were 89% and 79%, respectively (Table 2).

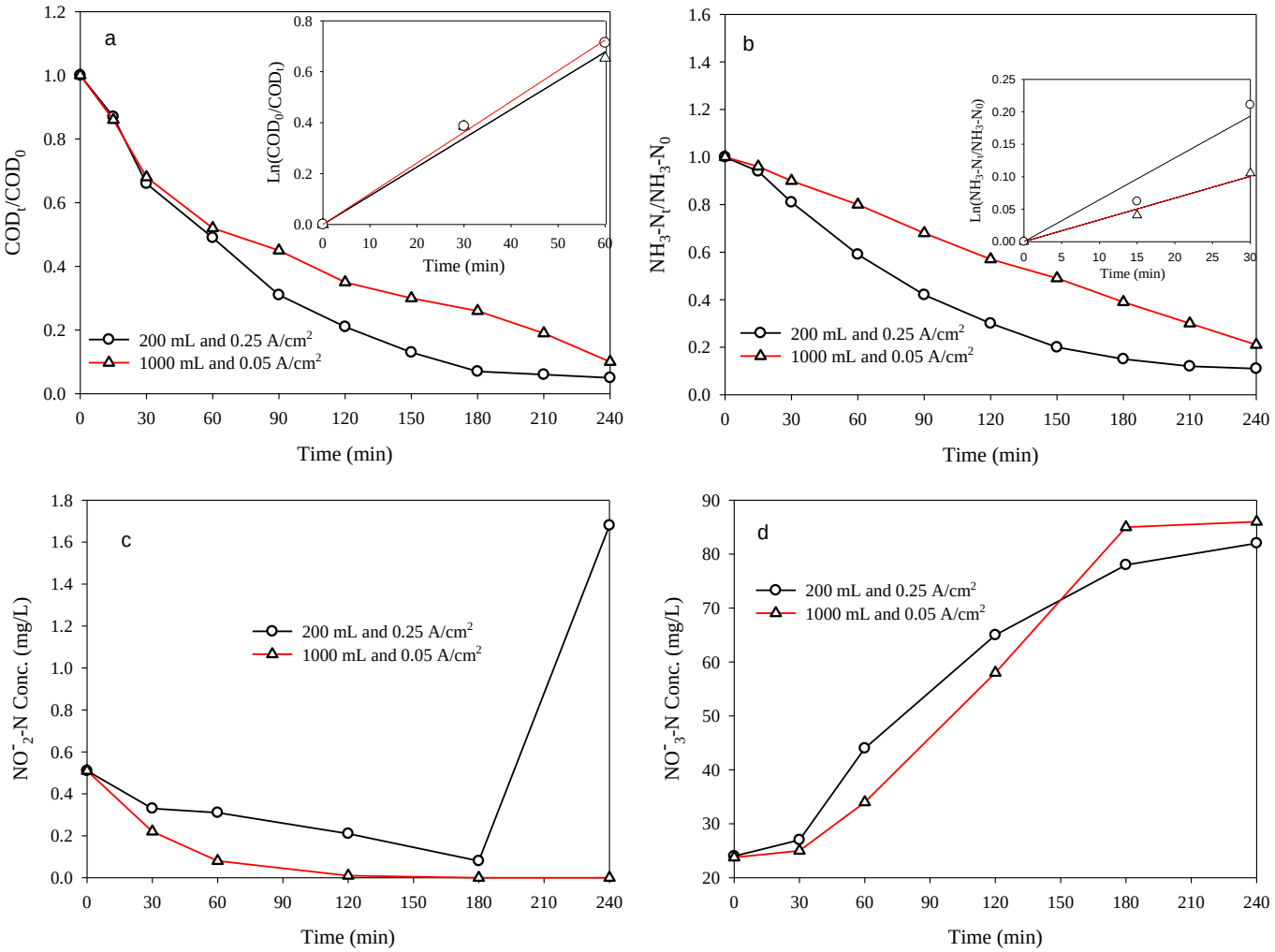

Figure 8. Concentration variations in COD (a), NH_3-N (b) NO_2^--N (c), and NO_3^--N (d) over time for different wastewater volumes and current densities during electrochemical treatment of swine wastewater (anode: BDD-I, d = 2.6 cm, and CA = 4 cm^2) (inset: Ln(C_o/C) against time, C = COD or NH_3-N).

The respective corresponding k values were 2.01×10^{-4} and 1.88×10^{-4} 1/s for COD degradation and 1.40×10^{-4} and 5.66×10^{-5} 1/s for NH_3-N removal (Table 2). Some researchers have also observed that organic pollutant degradation increases with increases in current density [11,19,35]. However, the E_{SP} at V_W = 1000 mL and C_D = 0.05 A/cm^2 was 32 kWh/kg-COD, which was significantly lower than that (213 kWh/kg-COD) at V_W = 200 mL and C_D = 0.25 A/cm^2, so the former operating condition could also be considered for energy or cost savings, regardless of the trend toward obtaining lower E_{SP} at higher initial COD concentrations, as shown in Tables 1 and 2. At V_W = 200 mL and C_D = 0.25 A/cm^2, the nitrite concentration decreased over time from 0–180 min and then increased over time up

to the end of the 240-min electrolysis. An analogous drift was also found at V_W = 1000 mL and C_D = 0.05 A/cm^2, but the nitrite concentrations were ND at t > 120 min (Figure 8c). During electrolysis, the nitrite concentrations in both tests increased over time; however, the nitrate concentration was higher at V_W = 200 mL and C_D = 0.25 A/cm^2 than it was at V_W = 1000 mL and C_D = 0.05 A/cm^2, principally due to the greater C_D in the former than in the latter although this trend was reverse at t > 150 min (Figure 8d).

4. CONCLUSIONS

In this study, the performance of our lab-prepared BDD anode was comparable to that of a commercial one for the electrochemical removal of COD and NH_3-N in swine wastewater. The performance tested anodes were in the following order: BDD-I ≈ BDD-II > graphite/PbO_2 ≈ Ti/PbO_2 > DSA for COD degradation, while they changed to graphite/PbO_2 ≈ Ti/PbO_2 > BDD-I ≈ BDD-II > DSA for NH_3-N removal. The COD and NH_3-N removal efficiencies increased with increases in the electrode distance. A similar tendency was also observed when increasing the cathode area, along with increases in nitrate production. A larger cathode area was also more beneficial for the control of the final pH. Greater COD and NH_3-N removal was also found at V_W = 200 mL and C_D = 0.25 A/cm^2 than at V_W = 1000 mL and C_D = 0.05 A/cm^2. However, the E_{SP} at V_W = 1000 mL and C_D = 0.05 A/cm^2 was 32 kWh/kg-COD, which was significantly lower than that (213 kWh/kg-COD) at V_W = 200 mL and C_D = 0.25 A/cm^2, so the former operating condition can also be considered for energy or cost savings, regardless of the trend toward a lower E_{SP} obtained at higher initial COD concentrations. The pseudo-first-order rate constants for the COD and NH_3-N removal ranged from 9.00×10^{-5}–5.98×10^{-4} and 5.66×10^{-5}–1.45×10^{-3} 1/s, respectively. The ranges of their R_E were 79%–100% and 72%–100%, respectively, while that of E_{SP} was 32–358 kWh/kg-COD.

ACKNOWLEDGEMENTS
The authors would like to thank the Ministry of Science and Technology, Taiwan for financially supporting this research under Grant No. MOST 106-2221-E-020-003-MY3. We are also grateful for the financial assistance of Prosperity Sci-Tech Co., Ltd. under a project (B10700245) financially supported by the Kaohsiung Environmental Protection Bureau.

References

1. E.R. Campagnolo, K.R. Johnson, A. Karpati, C.S. Rubin, D.W. Kolpin, M.T. Meyer, J.E. Esteban, R.W. Currier, K. Smith, K.M. Thu, M. McGeehin, *Sci. Total Environ.*, 299 (2002) 89–95.
2. T. Osada, M. Shiraishi, T. Hasegawa, H. Kawahara, *Front. Environ. Sci. Eng.*, 11(3) (2017) 10.
3. X. Song, R. Liu, L. Chen, B. Dong, T. Kawagishi, *Front. Environ. Sci. Eng.*, 11(3) (2017) 13.
4. United States Environmental Protection Agency (USEPA), Literature Review of Contaminants in Livestock and Poultry Manure and Implications for Water Quality, EPA 820-R-13-002, 2013.
5. K. Kumar, S.C. Gupta, Y. Chander, A.K. Singh, *Adv. Agron.*, 87 (2005) 1.
6. W. Ding, S. Cheng, L. Yu, H. Huang, *Chemosphere*, 182 (2017) 567.
7. F. Béline, J. Martinez, *Bioresour. Technol.*, 83 (2002) 225.

8. N. Montes, M. Otero, R.N. Coimbra, R. Méndez, J. Martín-Villacorta, *Environ. Technol.*, 36(15) (2015) 1966–1973.
9. S.Y. Sheen, C.M. Hong, M.T. Koh, C.C. Su, Swine waste treatment in Taiwan, http://www.fftc.agnet.org/htmlarea_file/library/20110802095125/eb381.pdf, accessed 09/01/2018.
10. B.M. Ha, D.T.G. Huong, *Geosci. Eng.*, LXIII(1) (2017) 15.
11. F.C. Moreira, R.A.R. Boaventura, E. Brillas, V.J.P. Vilar, *Appl. Catal. B: Environmental*, 202 (2017) 217.
12. J. Radjenovic, D.L. Sedlak, *Environ. Sci. Technol.*, 49(19) (2015) 11292.
13. I. Sirés, E. Brillas, M.A. Oturan, M.A. Rodrigo, M. Panizza, *Environ. Sci. Pollut. Res.*, 21 (2014) 8336.
14. L. Li, L. Liu, *J. Hazard. Mater.*, 161 (2009) 1010.
15. K.L. Huang, K.W. Wei, M.H. Chen, C.Y. Ma, *Int. J. Electrochem. Sci.*, 13 (2018) 11418.
16. T.S. Chen, K.L. Huang, Y.C. Pan, *Int. J. Electrochem. Sci.*, 7 (2012) 11191.
17. R.A. Pinheiro, C.M. de Lima, L.R.D. Cardoso, V.J. Trava-Airoldi, E.J. Corat, *Diam. Relat. Mater.*, 65 (2016) 198.
18. C. A. Martínez-Huitle, S. Ferro, *Chem. Soc. Rev.*, 35 (2006) 1324.
19. V. Punturat and K.L. Huang, *J. Taiwan Inst. Chem. Eng.*, 63 (2016) 286.
20. Y. He, W. Huang, R. Chen, W. Zhang, H. Lin, H. Li, *Sep. Purif. Technol.*, 156 (2015) 124.
21. T.S. Chen, P.H. Chen, K.L. Huang, *J. Taiwan Inst. Chem. Eng.*, 45 (2014) 2615.
22. G. Fóti, D. Gandini, Ch. Comninellis, A. Perret, W. Haenni, *Electrochem. Solid-State Lett.*, 2 (1999) 228.
23. Ch. Comninellis, *Electrochim. Acta*, 39 (1994) 1857.
24. T.A. Enache, A.M. Chiorcea-Paquim, O. Fatibello-Filho, A.M. Oliveira-Brett, *Electrochem. Commun.*, 11 (2009) 1342.
25. L. Szpyrkowicz, F. Naumczyk, F. Zilio-Grandi, *Water Res.*, 29 (1995) 517.
26. A. Kapałka, L. Joss, A. Anglada, Ch. Comninellis, K.M. Udert, *Electrochem. Commun.*, 12 (2010) 1714.
27. A. Fernandes, D. Santos, M.J. Pacheco, L. Ciríaco, A. Lopes, *Appl. Catal. B: Environmental*, 148/149 (2014) 288.
28. G. Pérez, R. Ibáñez, A.M. Urtiaga, I. Ortiz, *Chem. Eng. J.*, 197 (2012) 475–482.
29. V. Schmalz, T. Dittmar, D. Haaken, E. Worch, *Water Res.*, 43 (2009) 5260.
30. J.W. Peel, J.K.J. Reddy, B.P. Sullivan, J.M. Bowen, *Water Res.*, 37 (2003) 2512.
31. S. Garcia-Segura, M. Lanzarini-Lopes, K. Hristovski, P. Westerhoff, *Appl. Catal. B: Environmental*, 236 (2018) 546.
32. R. Zhao, X. Zhang, F. Chen, X. Man, W. Jiang, *Int. J. Environ. Res. Public Health*, 16 (2019) 343.
33. Y. Vanlangendonck, D. Cornisier, A. Van Lierde, *Water Res.*, 39 (2005) 3028.
34. G. Wang, C. Feng, C. Kang, B. Zhang, N. Chen, X. Zhang, *J. Environ. Eng.*, 142(2) (2016) 04015066.
35. S. Alcocer, A. Picos, A.R. Uribe, T. Pérez, J.M. Peralta-Hernández, *Chemosphere*, 205 (2018) 682.